Ion Transport in Glassy Polymer Electrolytes

C. T. Imrie, M. D. Ingram,* and G. S. McHattie

Department of Chemistry, University of Aberdeen, Meston Walk, Aberdeen AB24 3UE, Scotland

Received: October 6, 1998; In Final Form: January 26, 1999

The existence is reported of a new class of polymer electrolytes, containing polyether backbones and pendent mesogenic groups. These are amorphous (and sometimes liquid crystalline) polymeric solids with sub-T_g conductivities approaching 10^{-5} S cm^{-1} at ambient temperatures. The apparent decoupling of ion transport from structural relaxations in the host material implies the existence of a truly "solid" polymer electrolyte, which also implies a link between ion-transport mechanisms in glasses and in polymeric materials. In future it should be possible to develop materials for a variety of electrochemical applications, based on this new design strategy.

Introduction

It is generally accepted that since ion transport in polymer electrolytes (typically solutions of lithium salts in polyether systems) involves segmental motions of the host polymer,[1] significant levels of ionic conductivity will exist only above the glass transition temperature, T_g.[2,3] By contrast, in *inorganic* systems, ionic conduction is widespread in the glassy state, and in some "superionic" glasses[2,4,5] reaches values of 10^{-2} S cm^{-1} at ambient temperature.

These two differing patterns of behavior may be distinguished by means of Angell's decoupling index,[2,6] which in turn is based on ideas developed by Moynihan[7] to rationalize the contrasting conductivity and viscosity behaviors in glass-forming molten salts. Angell[2,6] defines the decoupling index R_τ at T_g, either as

$$R_\tau = \tau_H/\tau_\sigma \tag{1}$$

or as

$$R_\tau = \tau_s/\tau_\sigma \tag{2}$$

where τ_H and τ_S are enthalpic and shear relaxation times determined, respectively, by differential scanning calorimetry (DSC) and dynamic mechanical thermal analysis (DMTA), and τ_σ is a "conductivity relaxation time" extracted either from the frequency-dependent conductivities or from electric modulus spectroscopy.

If one focuses on eq 2, and considers the situation where the glass transition is detected by loss peaks in DMTA experiments at a frequency of 1 Hz (which is the standard frequency used in this paper), the (macroscopic) shear relaxation time is given by $\tau_S = 1/\omega_{max} = (2\pi)^{-1} = 0.159$ s. The corresponding electrical relaxation time is given by $\tau_\sigma = \epsilon_r\epsilon_0/\sigma$ (where ϵ_r and ϵ_0 are the relative permittivity and permittivity of free space, respectively) and σ is the conductivity. If, for convenience, ϵ_r is assumed to be about 12 in the moderately polar polyether electrolytes, then $\tau_\sigma \cong 10^{-12}/\sigma$.

It follows from the above that

$$R_\tau = \tau_s/\tau_\sigma \cong 0.159\sigma/10^{-12} = 1.59 \times 10^{11}\sigma \tag{3}$$

Equation 3 shows that the existence of even a modest conductivity (e.g. 10^{-6} S cm^{-1}) at the mechanically determined T_g implies a substantial degree of decoupling between the electrical and mechanical properties of the electrolyte.

If the T_g is determined by DSC, then τ_H is normally taken as 100 s [2,6] and

$$R_\tau = \tau_H/\tau_\sigma \cong 10^{14}\sigma \tag{4}$$

Generally, Angell and co-workers have used this latter method of evaluating R_τ values.

Thus, Angell and Torrell[3] conclude that whereas R_τ values in inorganic glasses are typically around 10^{11} (e.g. in silicate glasses) and even reach values of $10^{13}-10^{14}$ in certain superionic glasses, values *less than 1* may be expected for common "salt in polyether" polymer electrolytes. (Values lower than unity are obtainable because ionic mobility is being further reduced by ion-pairing.[3])

The prevailing strategy for optimizing the conductivity of solvent-free polymer electrolytes[8−10] is indeed based (a) on speeding up segmental motions by lowering T_g; and (b) on reducing the tendency towards the formation of ion pairs. An alternative approach which certainly leads to attractive conductivities even at ambient temperatures is to add high levels of organic solvent (e.g. propylene or ethylene carbonate) to suitable polymers (e.g. poly(methyl methacrylate) to produce "ionic gels". These are being used increasingly for a variety of electrochemical applications.[11−13]

By contrast, there are only a few reports in the literature[14−17] of significant levels of ionic conductivity being encountered in polymers below T_g. In some cases, these refer to the poly(vinyl alcohols)[15,16] where, we suppose, hydrogen bonding and/or protonic transport may (or may not) have an influence on the behavior observed. There is thus little discussion of the phenomenon of "superionic" conductivity in polymer materials, and so a distinction has remained between the inorganic glasses, which show "decoupled" conductivity mechanisms, and the

* To whom correspondence should be addressed.

10.1021/jp983968e CCC: $18.00
Published on Web 03/13/1999

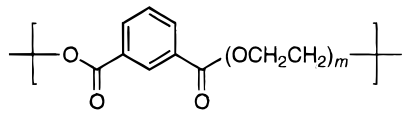

m = 4, 6, 13, 20, 34

(a)

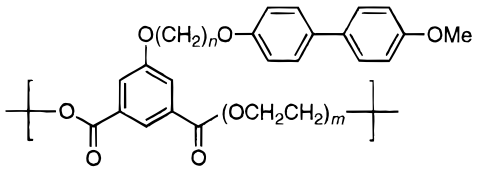

n = 3, 4, 5, 6, 12: m = 4, 6, 13, 20, 34

(b)

Figure 1. Molecular structures of polymers under investigation: (a) the 0G*m* series, where 0 indicates the absence of pendent side chains and *m* is the number of ethylene oxide (EO) units per repeat unit; (b) the MeOC*n*G*m* series, where *n* is the number of CH_2 spacers separating the mesogenic groups from the polymer backbone.

polymer electrolytes where ionic and segmental motions are strongly coupled to each other.

The recent discovery by Angell et al.[18,19] of "polymer-in-salt" systems, where polymers are added in order to gelatinize low-temperature molten salts does not significantly change this situation. These latter systems are effectively "solvent-free gels", where the essential decoupling of ionic motions from the host matrix occurs in the molten salt even in the absence of polymer.

In this paper, we present clear evidence for the existence of decoupled ion transport in solvent-free glassy polymer electrolytes. We approach this problem through the synthesis of a new family[20] of side-group liquid-crystal polymer electrolytes (sglcpe's), where mesogenic side groups impose a characteristic ultrastructure on both the polymeric molecule and to a lesser extent, on the polyether backbone. This family of sglcpe's is defined by the range of molecular formulas shown in Figures 1, a and b. Figure 1a shows a polymer based on the largely ethylene oxide backbone, without pendent mesogenic groups attached. Figure 1b shows the method of attachment of the calamitic 4-methoxybiphenyl mesogens by means of alkoxy spacers. It is possible to vary independently the number of CH_2 groups, *n*, in these alkoxy spacers, and the number of ethylene oxide (EO) repeat units, *m*, in the EO "chainlets" which are stitched together by isophthalic ester linkages. The properties of this family of polymers are strongly influenced by the presence of the side groups and by the values of *n* and *m*.

It is emphasized here that somewhat analogous sglcpe systems were recently described by Wright and co-workers.[21,22] However, in those studies the pendent side groups were simple alkyl chains, and the resulting salt−polymer complexes tended to crystallize on cooling. This crystallization process obscured the glass transition phenomena and we suggest almost certainly precluded observation of the effects described in the present paper.

Experimental Techniques

The syntheses of representative members of the 0G*m* and MeOC*n*G*m* series have been described in detail elsewhere.[20] The proposed structures of all the intermediates and polymers have been verified using ^1H and ^{13}C NMR and IR spectroscopy. The molecular weights of the polymers were estimated using gel permeation chromatography using a Knauer Instruments chromatograph containing two PL gel 10 μm mixed columns and interfaced to a PC operating Polymer Laboratories GPC SEC V5.1 software. Calibration was performed using polystyrene standards with chloroform as the eluent.

The polymer−$LiClO_4$ complexes were prepared by codissolving appropriate amounts of the polymer and dry $LiClO_4$ in anhydrous THF. The complex was solvent cast directly onto a stainless steel electrode and the THF allowed to evaporate under a stream of argon. Residual traces of THF were removed by drying under vacuum for several days. The concentration of lithium ions in the complex is described as the ratio of active oxygens to lithium ions. An active oxygen is defined in terms of its ability to coordinate the lithium ion which is influenced both by steric factors and donicities of individual oxygens. Rather arbitrarily, we have assumed that all the oxygen atoms in the polymer backbone may be counted except for the carbonyl oxygens. Thus both the 0Gm and MeOCnGm series contain $(m + 1)$ active oxygens per repeat unit.

The thermal characterization of the polymers and their salt complexes was performed by differential scanning calorimetry (DSC) and dynamic mechanical thermal analysis (DMTA). Two DSCs were used for these studies: a Polymer Laboratories PL-DSC equipped with a liquid nitrogen autocool accessory and a Mettler-Toledo 821 DSC equipped with a refrigerant cooling system. Both instruments were calibrated using indium as a standard. Each sample was cooled to ca. −70 °C, held at that temperature for 3 min, heated to 120 °C, held for 3 min, cooled, and the cycle repeated. All heating and cooling rates were 10 °C min^{-1}. The DMTA measurements were made using a PC-controlled Rheometric Scientific DMTA equipped with a MK111 analyzer operating in the shear mode. Each sample was loaded into the drive shaft head, cooled to −70 °C, and reclamped to ensure good clamp−sample contact. Measurements were recorded at a heating rate of 2 °C min^{-1} up to a maximum temperature of 120 °C. Phase identification was performed by polarized light microscopy using an Olympus BH2 polarized light microscope equipped with a Linkam THMS heating stage, LNP2 cooling pump, and TMS control unit.

Ionic conductivities of the polymer−salt complexes were measured by standard ac impedance methods using a Schlumberger 1260 impedance analyzer over a frequency range $1-10^6$ Hz. The sample was pressed between stainless steel electrodes under an anhydrous argon atmosphere. Complex impedance plots were obtained using Zview software.

Results

Behavior of the "Backbone" Polymers. The polymers under investigation are those in the 0G*m* series depicted in Figure 1a, where pendent side groups are absent, and *m* can have values of 4, 6, 13, 20, and 34. The corresponding values of the degree of polymerization, *p*, are nominally 9, 21, 20, 17, and 10, respectively. On cooling 0G13, 0G20, and 0G34 from the isotropic phase, a spherullitic texture develops when viewed through the polarized light microscope. For 0G34 the optical texture is identical to that observed for high molecular weight poly(ethylene oxide). Thus these polymers are crystalline in nature. By comparison, 0G4 and 0G6 and all the 0gm−salt complexes are amorphous at all temperatures.

Values of glass transition temperature, T_g, and of melting temperature, T_m, are shown in Figure 2 for pure polymer and for the $LiClO_4$ complex of AO:Li = 10:1 composition. In the absence of $LiClO_4$, partially crystalline samples are obtained for $m \geq 13$, and both the degree of crystallinity and the melting

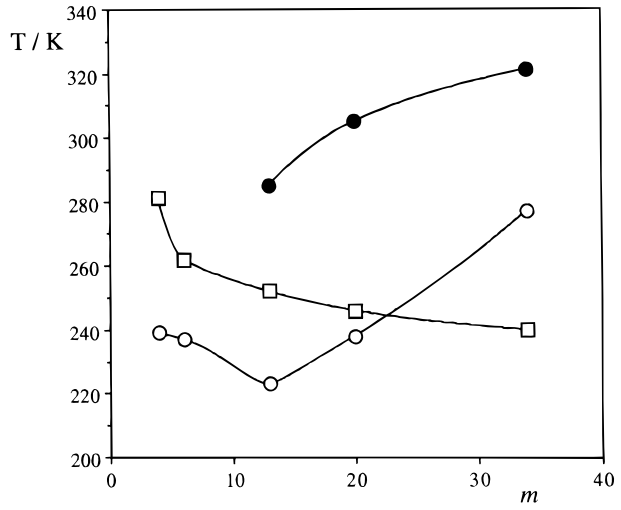

Figure 2. Thermal properties of polymers and their complexes with $LiClO_4$ in the 0G*m* series, plotted as a function of *m*. Symbols are (○) T_g, polymer only; (●) T_m, polymer only; (□) T_g, polymer-salt complex (AO: Li ratio = 10:1, see text).

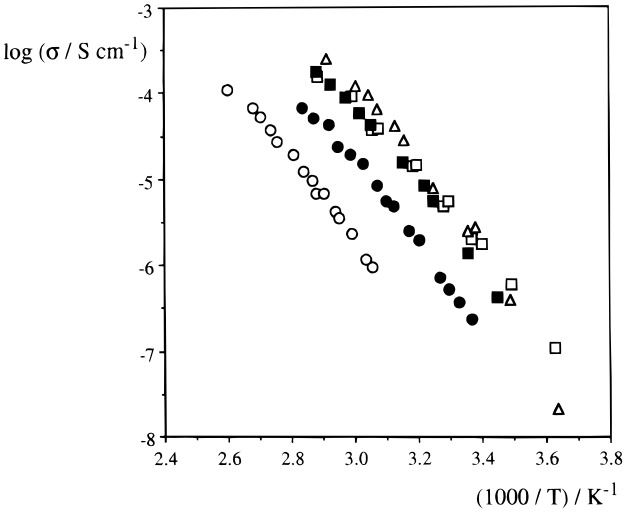

Figure 3. Arrhenius plots of ionic conductivities of the $LiClO_4$ complexes (AO: Li = 10:1) for polymers in the 0G*m* series, as in Figure 2. Symbols are (○) $m = 4$; (●) $m = 6$; (□) $m = 13$; (■) $m = 20$; (△) $m = 34$.

point increase with increasing length of EO chainlets. The values of T_g, by contrast, initially decrease with increasing *m*, and then increase in parallel with the increase in T_m.

Addition of $LiClO_4$ suppresses crystallization and leads to simpler T_g behavior. The effect of lengthening the chainlets (which moves the isophthalic moieties further apart) is to lower the value of T_g.

The conductivities of these $LiClO_4$ complexes are presented in the form of Arrhenius plots in Figure 3. The conductivities at $10^3/T = 3.33$ K^{-1} (i.e., at 300 K) lie in the range approximately 3×10^{-7} to 3×10^{-6} S cm^{-1}, which is unremarkable behavior for nonplasticized EO-based polymer electrolytes.[9] It is clear, however, that short EO chainlets are associated with low conductivity levels and that the ester linkages are having an adverse effect on ion mobility, and this parallels the rise in T_g.

Behavior of Polymers with Pendent Side Chains. The polymers under investigation here are those in the MeOC6G*m* series depicted in Figure 1b, having always the same pendent groups ($n = 6$), and *m* values of 4, 6, 13, 20, and 34 as described in the previous section. MeOC6G20 and MeOC6G34 exhibit

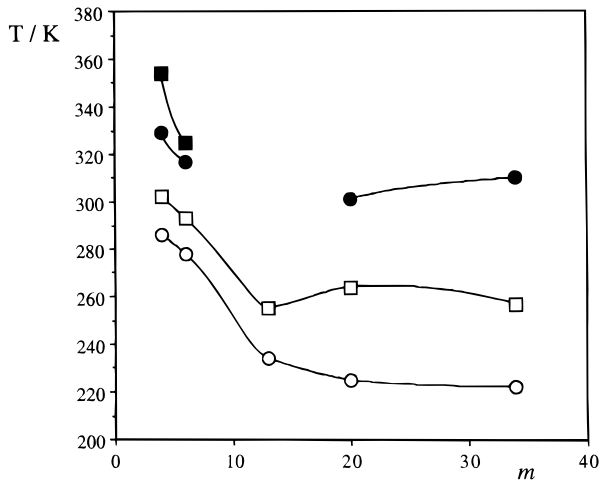

Figure 4. Thermal properties of polymers and their complexes with $LiClO_4$ in the MeOC6G*m* series, plotted as a function of *m*. Symbols are (○) T_g, polymer only; (●) T_m, polymer only; (□) T_g, polymer−salt complex; (■), T_m, polymer−salt complex (AO: Li ratio = 10:1, see text).

spherullitic optical textures similar to those described for members of the 0G*m* series ($m = 13$, 20, 34) and hence these are assigned as crystalline polymers. On cooling MeOC6G4 and MeOC6G6 slowly from the isotropic phase, a finely grained birefringent texture developed. This resembled a poorly defined focal conic fan texture but it was not possible to obtain a clear characteristic texture using which an unambiguous phase assignment could be made. The observation of focal conic defects, however, implies a layered smectic structure and preliminary X-ray diffraction measurements support this view. MeOC6G13 was amorphous at all temperatures. The MeOC6G*m*−salt complexes with $m = 13$, 20, and 34 were amorphous while $m = 4$ and 6 exhibited smectic behavior although, as before, an unambiguous phase assignment was not possible.

Figure 4 shows the thermal behaviors as revealed by DSC. The presence of side chains leads to a pattern of melting behavior more complex than that seen in Figure 2. In the absence of $LiClO_4$, two types of melting behavior are seen. First, there is the "clearing endotherm" for the liquid crystalline phase in short-chainlet polymers (i.e., $m = 4$ and 6), and second, there is the normal melting point for the longer EO chainlets, seen when $m = 20$ and 34. In the presence of $LiClO_4$, the crystallization of EO chainlets is suppressed (as happened also in the absence of the side chains), but the liquid-crystalline clearing temperatures are still observed.

Table 1 summarizes the DSC data for polymers and polymer−salt complexes in the 0G*m* and MeOG*m* series. Values of ΔH for the first-order transitions (T_c and T_m) are calculated per mole of repeat unit, so the molecular weight will automatically increase on going from the 0G*m* to MeOC6G*m* series and with increasing values of *m* down either series. Effectively, therefore, one should be careful to make only "horizontal" comparisons, i.e., across the table at constant values of *m*.

Nevertheless, one can see from Table 1 how the presence of the pendent side groups introduces liquid crystalline effects at the lowest *m* values (4 and 6) and that the degree of this liquid crystalline order (as indicated by ΔH) is not greatly diminished by the presence of $LiClO_4$ salt at the AO:Li ratio of 10:1. Information from these thermal measurements is supported by the optical microscopy, which shows evidence for a smectic phase in these low *m*-value polymers and polymer−salt complexes.

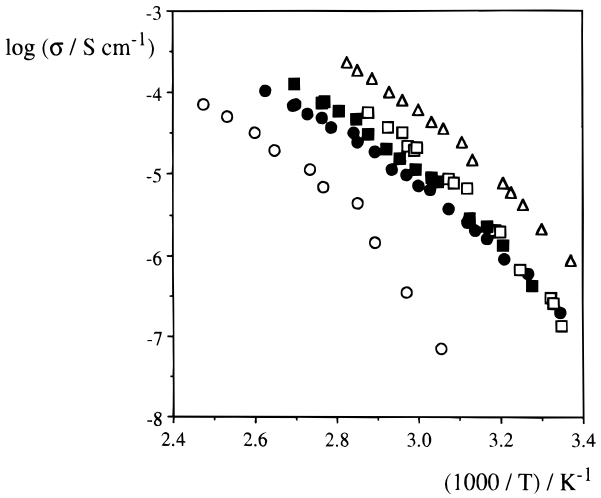

Figure 5. Arrhenius plots for conductivities of the $LiClO_4$ complexes (AO:Li = 10:1) for polymers in the MeOC6G*m* series, as in Figure 4. Symbols are the same as in Figure 3.

TABLE 1: Thermal Properties of Polymers and Polymer−$LiClO_4$ Complexes (RO:Li = 10) in the 0G*m* and MeOC6G*m* Series

	0G*m* polymers			MeOC6G*m* polymers		
m	T_g (K)	T_m (K)	ΔH (kJ mol^{-1})	T_g (K)	T_m*/T_c (K)	ΔH (kJ mol^{-1})
4	239			286	329	15.3
6	237			278	317	15.3
13	223	285	28.8	234		
20	238	305	83.7	225	301*	72.7
34	277	321	161.1	222	310*	149.8
	0G*m*:$LiClO_4$ complexes			MeOC6G*m*:$LiClO_4$ complexes		
m	T_g (K)	T_m (K)	ΔH (kJ mol^{-1})	T_g (K)	T_c (K)	ΔH (kJ mol^{-1})
4	281			302	354	11.1
6	262			293	325	10.5
13	250			255		
20	245			264		
34	241			257		

At larger *m* values, $m = 20$ and 34, the thermal behavior is dominated by the melting of crystalline EO chainlets. This melting process is effectively suppressed by the addition of salt (which complexes directly to the EO segments[23]) and is also influenced (but to a lesser extent) by the presence of the pendent side groups. Thus, even at $m = 34$, when side groups are present, one can observe some decrease in the ΔH value corresponding to the melting of the EO chainlets.

Inspection of Figure 4 and Table 1 shows that the glass transition behavior by contrast is apparently simplified by the presence of side groups, where T_g values fall away almost continuously with increasing chainlet length. Comparing the values in Table 1, for polymers with and without side chains, the effect of these pendent groups in increasing T_g is only seen at lower *m* values ($m = 4-13$).

In effect, and depending on the value of *m*, there are two types of polymer electrolyte behavior. For small values ($m = 4$ and 6), the properties are strongly influenced by the side chains and the materials in question may fairly be termed sglcpe's. In contrast, for large values ($m = 20$ and 34) "conventional polymer electrolyte behavior" is observed. Intermediate behavior is found for $m = 13$.

The conductivities of the polymer-salt complexes are presented as Arrhenius plots in Figure 5. The conductivities at $10^3/T = 3.33$ K^{-1} (i.e., at 300 K) now lie in the range approximately $10^{-9}-10^{-6}$ S cm^{-1}, which is a wider spread than is found in the absence of side groups. Compare Figures 3 and 5. It is clear that the smallest conductivities in Figure 5 are found for the smallest *m* values, i.e., when the side groups are brought closest together. The largest conductivities are found for the largest *m* values, where "normal" polymer electrolyte behavior is approached. Notwithstanding this adverse trend in conductivity, the interest now centers on the behavior seen at the *small* values of m. First, when $m = 4$, there is an apparent kink (or knee) in the Arrhenius plot at $10^3/T \cong 2.85$ K^{-1}, i.e., at $T \cong 350$ K, which almost coincides with $T_c = 354$ K as determined by DSC. The Arrhenius plot is steeper below T_c (i.e., E_A is larger), which suggests that the onset of liquid crystallinity is bad for ionic conductivity in this case.

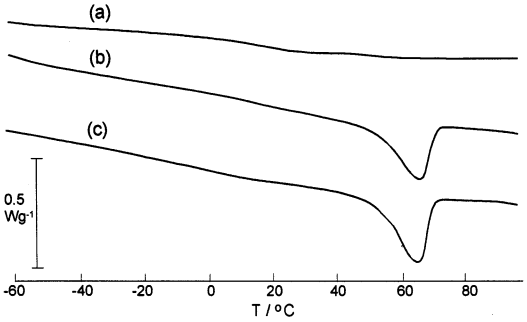

Figure 6. DSC traces for $LiClO_4$ complexes of the MeOC6G6 polymer, at different AO:Li ratios: (a) 3:1, (b) 7.5:1, and (c) 10:1. Note the progressive growth of the endothermic event corresponding to T_c (see text), in the sequence (a) < (b) < (c).

However, when $m = 6$, where a liquid crystalline phase is still present, the knee is not present in the Arrhenius plot, and much higher conductivities are observed at low temperatures. Although this material is effectively solid at room temperature ($T_g = 320$ K), the corresponding conductivity (ca. 3×10^{-6} S cm^{-1}) is appreciable and suggests a strongly decoupled transport mechanism. This system was chosen for more detailed investigation.

Influence of $LiClO_4$ Content on Ionic Conductivity. The polymers in question are those in the MeOC6G6 system, and comparisons are made between the properties of the $LiClO_4$ complexes of this polymer with AO:Li ratios of 10:1, 7.5:1, and 3:1. The corresponding molalities are 0.98, 1.31, and 3.28 mol kg^{-1}, respectively.

The thermal properties are summarized in Figure 6. The increasing suppression of the T_c endotherm which is seen at high salt concentrations is probably indicative of the much slower formation of the liquid crystalline phase in the presence of salt, on the time scale of the DSC experiment. This increasing tendency toward amorphicity is accompanied by a substantial increase in conductivity, see Figure 7. At approximately 300 K, the conductivity increases by a factor of 300, i.e., from 10^{-7} to approximately 3×10^{-5} S cm^{-1}, as the $LiClO_4$ concentration is increased by a factor of 3.3. For the most concentrated, and also the most highly conducting salt−polymer complex, an activation energy of 26 kJ mol^{-1} may be calculated, which is also evidence for a fairly "fast" ion transport mechanism.

These $LiClO_4$−MeOC6G6 complexes have been further investigated by DMTA. Changes from glassy to liquid crystalline or from liquid crystalline to isotropic liquid behavior are indicated by changes in the shear modulus G' which will be accompanied by peaks in the loss tangent, δ. Experimental results are given in Figure 8a,b. Clearly, the 10:1 and 7.5:1

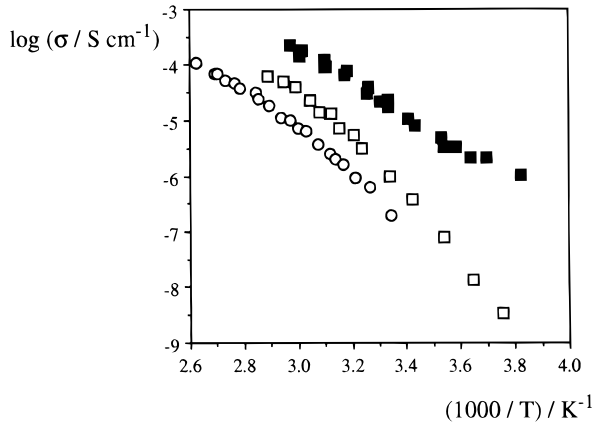

Figure 7. Arrhenius plots for conductivities of the $LiClO_4$ complexes for the polymer MeOC6G6, as in Figure 6. Symbols are (○) 10:1; (□) 7.5:1; and (■) 3:1.

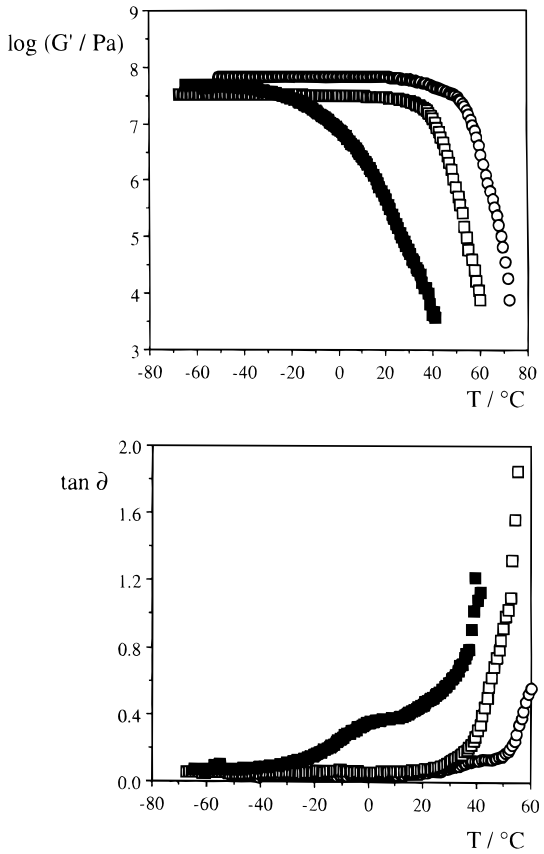

Figure 8. (a, top) Temperature dependence of the real (storage) component of the shear modulus of the $LiClO_4$-MeOC6G6 complexes (symbols as in Figure 7). (b, bottom) Corresponding temperature dependence of the imaginary (loss) component of the shear modulus of the $LiClO_4$−MeOC6G6 complexes (symbols as in Figure 7).

complexes behave very similarly. Both are solids up to and beyond ambient temperatures, and the observed liquid crystalline range is very short indeed (perhaps only 10 K). In the 3:1 complex there is little sign of crystallinity, but the glass transition phenomenon is more clearly evident in the mechanical loss spectrum, see Figure 8b.

Discussion

A straightforward comparison of the electrical and mechanical properties, (Figures 7 and 8) reveals that at least two $LiClO_4$−polymer complexes, i.e., those with the 10:1 and 7.5:1 stoichiometries, respectively, have been synthesized which are good ionic conductors in the solid state. This is the result which was being sought, but the question arises as to what is means.

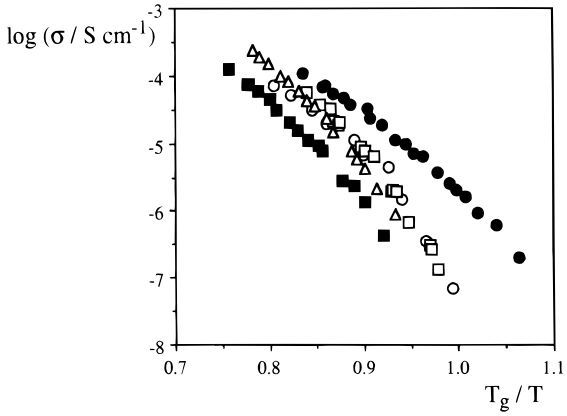

Figure 9. "Scaled" Arrhenius plots for $LiClO_4$−polymer complexes in the MeOC6G*m* series, where the abscissa (T_g/T) is the inverse temperature scaled with respect to the (DMTA) glass transition. Data and symbols are the same as in Figure 3.

The polymers under investigation are fairly conventional ethylene−oxide based systems, so why has this phenomenon been little remarked until now, given that well-prepared strategies[8−10] have been consistently applied to optimize the conductivities of these systems? The answer, very probably, is that we have pursued an approach to polymer design which runs exactly counter to these accepted strategies. Where, before, the aim had been to loosen the polymer segments (i.e., lowering T_g) and to incorporate additional ion-solvating groups, we instead have *stiffened* the backbone by the inclusion of isophthalic ester linkages and have added *nonsolvating* side groups.

The effect of this unusual strategy is that we have been able to build polymers with self-organized ultrastructures which exist in the absence of dissolved salt. These structures prevent the cations from interacting too strongly with the EO chainlets, and thus from "building cages" in which they can become trapped especially at lower temperatures. Indeed the phenomenon of vitrification within these complex structures has the effect not of immobilizing the ions within these cages, but rather of stabilizing the ethylene oxide structure in a more open configuration, where there is excess volume and *empty sites* are available for the ions to move into. This in effect is a "glassy" mechanism,[24,25] regardless of whether the conduction is predominantly anionic or cationic, or if indeed it involves all the ions and charged particles dissolved in the host matrix.

To quantify the extent of decoupling in these polymers it is convenient to replot the conductivity data as a function of scaled inverse temperature (T_g/T), where in this case the T_g values are determined by DMTA. (Note that thermal manifestations of T_g tend to be rather weak in these systems.) Figures 9 and 10 show such *scaled* Arrhenius plots for two series of polymers: (a) those with increasing *m* values (MeOC6G*m*), and (b) for the MeOC6G6 polymer with differing $LiClO_4$ content. Apart from polymers where *m* is either 20 or 34, there is some evidence of decoupling in *all* the systems studied. The most decoupled system is the 7.5:1 complex of the MeOC6G6 polymer, where $\sigma(T_g) \cong 10^{-5}$ S cm^{-1}, and so from eq 3, $R_\tau \cong 1.6 \times 10^6$ at T_g.

Decoupling indices calculated in this way are given in Tables 2 and 3 for all the systems discussed in this paper. The value shown in parentheses implies that for this electrolyte the conductivities were just too small to be measured at T_g and some extrapolation of the data was required.

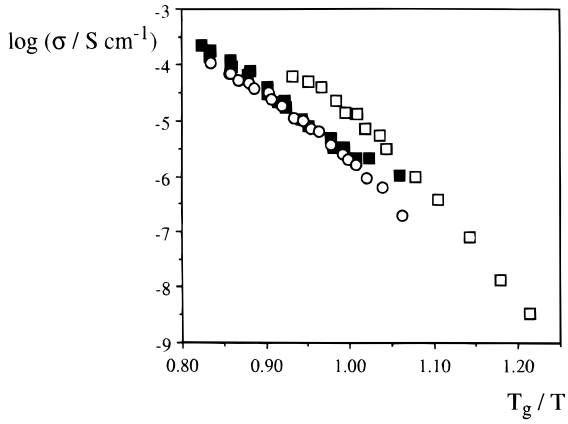

Figure 10. Scaled Arrhenius plots of $LiClO_4$ complexes of the MeOC6G6 polymer, where the inverse temperatures are scaled as in Figure 9. Data and symbols are same as in Figure 7.

TABLE 2: DMTA Loss Peaks and Decoupling Indices for $LiClO_4$ Complexes (AO:Li = 10) in the 0G*m* and MeOC6G*m* Series

	0G*m*:$LiClO_4$ complexes		MeOC6G*m*:$LiClO_4$ complexes	
m	T_g (DMTA) (K)	$R_\tau = \tau_s/\tau_\sigma$	T_g (DMTA) (K)	$R_\tau = \tau_s/\tau_\sigma$
4	306	1.0×10^4	(325)	1.0×10^4
6	283	5.0×10^5	318	5.0×10^5
13	254	1.0×10^2	292	(1.0×10^3)
	277	1.0×10^4		
20	262		281	
34	265		277	

TABLE 3: DMTA Loss Peaks and Decoupling Indices for $LiClO_4$ Complexes of the MeOC6G6 Polymer

AO:Li ratio	T_g (DMTA)	$R_\tau = \tau_s/\tau_\sigma$
3.0:1	277	3×10^5
7.5:1	323	1.6×10^6
10.0:1	318	5×10^5

What is remarkable is that R_τ values greater than unity are observed in both series, provided that the isophthalic ester groups in the EO backbones are not too far apart. It seems, therefore, that it may not be essential to incorporate mesogenic groups in order to promote decoupling. Stiffening of the polymer backbone to inhibit the coiling of the PEO helix also has an effect on the mechanism of ion solvation.

An interesting effect is observed with the 0G13 complex, where side groups are absent and each EO chainlet contains 13 segments. Here the DMTA trace revealed the existence of two relaxations. It is possible that this polymer shows intermediate character and separates into "stiff" and "loose" regions (with high and low T_gs, respectively). This splitting could give rise to two different decoupling indices.

Notwithstanding structural complexities, a common pattern of behavior is beginning to emerge, which embraces the sglcpe's discussed here, the amorphous poly(vinyl alcohol) reported by Yamomoto et al.[15] and Every et al.,[16] and the partially crystalline poly(vinylene carbonate) systems studied by Wei and Shriver.[17] In all these systems, appreciable conductivity is apparently observed in the solid state (especially at low ionic concentrations). Also, and in marked contrast to "normal" polymer electrolyte behavior, T_g (or T_m[17]) diminish and ionic mobility increases at high salt concentrations.

In this sense, all these systems are irregular in two (possibly distinct) ways. At low concentrations, decoupled ion transport is occurring within a rigid polymer framework. At high concentrations, it is not clear if the observed degree of decoupling originates in the same way, or if it is instead a manifestation of the "polymer in salt" behavior, described elsewhere by Angell *et al.*[18] More detailed studies using a wider variety of polymer−salt combinations will be necessary to establish this latter point. Either way, the consequential shifting of the maximum conductivity to higher salt concentrations is a very favorable outcome.

This new class of electrolytes could find applications in electrochemistry. The more concentrated polymer electrolytes would be especially adapted for use in lithium batteries, where even the adverse effects of low Li^+ ion transport numbers[26,27] (leading to concentration polarization) would be offset by diffusive transport of ion pairs to and from the electrodes. Furthermore, since the "self-trapping" effect is driven largely by the strong O:Li^+ interaction, and this self-trapping is apparently inhibited, it is likely that the cationic transport numbers will be larger in these decoupled systems.

Finally, we remark on the absence of a detectable change in slope in the Arrhenius plots (i.e., in Figures 5, 7, 9, and 10) on passing through the glass transition. Normally, in decoupled systems,[28] E_A is significantly greater above T_g than below and this difference is taken to indicate the unfreezing of melt structures. As the temperature changes, especially in *fragile* systems,[10,29] the structure of the melt is changing. The polymer electrolyte systems described in this paper, however, are expressly designed so as to confer a degree of "structural stability", and it is unsurprising that in their molten state they exhibit little sign of "fragile" behavior. This absence of fragility is manifested in the remarkable continuity between liquid and glassy behaviors.

Conclusion

Contrary to the accepted wisdom, it is now apparent that ionic transport can occur in certain polymeric glasses below T_g. We report the occurrence of this phenomenon in ethylene oxide based materials, where some degree of ultrastructure is imparted: either by the attachment of pendent mesogenic groups or more simply by introducing isophthalic ester linkages into the ethylene oxide chains. It is suggested that the presence of this kind of ultrastructure reduces the fragility of the liquid polymers and thereby inhibits the self-trapping of ions which normally becomes increasingly important on cooling toward T_g.

This is a very simple strategy worthy of further investigation. At present, it is not known how widespread is sub-T_g conduction in polymers (compare refs 15−17), nor is it known how far this decoupled form of ion transport involves both cations and anions. Wide-ranging and more detailed studies of this phenomenon are required.

Acknowledgment. One of us (G.S.M.) thanks the University of Aberdeen for financial support. The authors are indebted to G. Gordon Cameron (Aberdeen) and Peter V. Wright (Sheffield) for helpful discussions.

References and Notes

(1) Druger, S.; Ratner, M. A.; Nitzan, A. *Solid State Ionics* **1986**, *18−19*, 106.
(2) Angell, C. A. *Solid State Ionics* **1983**, *9−10*, 3; **1986**, 18−19, 72.
(3) Torell, L. M.; Angell, C. A. *Br. Polym. J.* **1988**, *20*, 173.
(4) Grant, R. J.; Ingram, M. D.; Turner, L. D. S.; Vincent, C. A. *J. Phys. Chem.* **1978**, *82*, 2838.
(5) Ingram, M. D. *Current Opinion in Solid State & Materials Science* **1997**, *2*, 399.
(6) Angell, C. A. *Chem. Rev.* **1990**, *90*, 523.
(7) Howell, F. S.; Bose, R. A.; Macedo, P. B.; Moynihan, C. T. *J. Phys. Chem.* **1974**, *78*, 639.

(8) Armand, M. B. *Solid State Ionics*, **1994**, *69*, 309.
(9) Meyer, W. H. *Adv. Mater*. **1998**, *10*, 439.
(10) Angell, C. A.; Imrie, C. T.; Ingram, M. D. *Polymer Int*. **1998**, *47*, 9.
(11) Bohnke, O.; Frand, G.; Rezrazi, M.; Rousselot, C.; Trouche, C. *Solid State Ionics* **1993**, *97*, 105.
(12) Cazzanelli, E.; Mariotto, G.; Appetecchi, G. B.; Croce, F.; Scrosati, B. *Electrochim. Acta* **1995**, *40*, 2379.
(13) Ingram, M. D.; Pappin, A. J.; Delalande, F.; Poupard, D.; Terzulli, G. *Electrochim. Acta* **1998**, *43*, 1151.
(14) Meyer, W. H. In *Polymer Electrolytes II*; MacCallum, J. R., Vincent, C. A., Eds.; Elsevier Applied Science; London, 1989; p 191.
(15) Yamamoto, T.; Inami, M.; Kanabara, T. *Chem. Mater*. **1994**, *6*, 44.
(16) Every, H. A.; Zhou, F.; Forsyth, M.; MacFarlane, D. R. *Electrochim. Acta* **1998**, *43*, 1465.
(17) Wei, X.; Shriver, D. F. *Chem. Mater*. **1998**, *10*, 2307.
(18) Angell, C. A.; Liu, C.; Sanchez, E. *Nature* **1993**, *362*, 137.
(19) Angell, C. A.; Xu, K.; Zhang S.-S.; Videa, M. *Solid State Ionics* **1996**, *86*−*88*, 17.
(20) McHattie, G. S.; Imrie, C. T.; Ingram, M. D. *Electrochim. Acta* **1998**, *43*, 1151.
(21) Dias, F. B.; Batty, S. V.; Ungar, G.; Voss, J. P.; Wright, P. V. *J. Chem. Soc., Faraday Trans.* **1996**, *92*, 2599.
(22) Dias, F. B.; Batty, S. V.; Gupta, A.; Ungar, G.; Voss, J. P.; Wright, P. V. *Electrochim. Acta* **1998**, *43*, 1217.
(23) Cameron, G. G.; Ingram, M. D.; Qureshi, M. Y.; Russell, G. M.; Wood, G. I. *Polym. Int.* **1994**, *33*, 347.
(24) Bunde, A.; Ingram, M. D.; Maass, P. *J. Non-Cryst. Solids* **1994**, *172*−*174*, 1222.
(25) Reference 24 introduced the concept of $\bar{C}$ sites (i.e. empty cation sites) as being essential to cation transport in glassy materials. The argument now is that empty "ion sites" in these structured polymers underpin the analogous transport mechanism.
(26) Cameron, G. G.; Harvie, J. L.; Ingram, M. D. *J. Chem. Soc., Faraday Discuss*. **1989**, *88*, 55.
(27) Bruce, P. G.; Vincent, C. A. *J. Chem. Soc., Faraday Discuss*. **1989**, *88*, 43.
(28) Ingram, M. D. *Phys. Chem. Glasses* **1987**, *28*, 215.
(29) Angell, C. A. *J. Non-Cryst. Solids* **1991**, *131*−*133*, 13.